



Rice paper as a separator membrane in lithium-ion batteries

L.C. Zhang, X. Sun, Z. Hu, C.C. Yuan, C.H. Chen*

CAS Key Laboratory of Materials for Energy Conversion, Department of Materials Science and Engineering, University of Science and Technology of China, Anhui, Hefei 230026, China

ARTICLE INFO

Article history:

Received 31 March 2011
Received in revised form 8 December 2011
Accepted 12 December 2011
Available online 19 December 2011

Keywords:

Rice paper
Lithium-ion battery
Separator
Membrane
Electrochemical window

ABSTRACT

A commercial rice paper (RP) is used for the first time as a separator membrane in lithium-ion batteries. It consists of interpenetrating cellulose fibers with a diameter of about 5–40 μm to form a highly porous structure. The RP is found to be electrochemically stable at a potential below 4.5 V vs. Li^+/Li . Several kinds of electrode materials including graphite, LiFePO_4 , LiCoO_2 and LiMn_2O_4 are used to test the compatibility of the RP in Li-ion batteries and to compare with a commercial polypropylene/polyethylene/polypropylene separator membrane. The RP separator with the same thickness gives rise to a lower resistance than the commercial separator. Due to the wonderful flexibility, high porosity, low cost and excellent electrochemical performance of the RP membrane, it is promising to partially replace commercial separators in lithium-ion batteries for low power applications.

© 2011 Elsevier B.V. All rights reserved.

1. Introduction

It has been 20 years since the appearance of the first commercial lithium-ion batteries. A lithium-ion cell is comprised of four components, i.e. a positive electrode, a negative electrode, a separator membrane and an electrolyte. Among them, the separator is a thin porous membrane which is placed between the positive and the negative electrodes to avoid a direct contact (i.e. short-circuiting) of the two electrodes. It allows free ionic transport but isolates electronic flow. There are mainly three kinds of separators [1] including micro-porous polymer membranes [2–4], non-woven fabric mats [5–11] and inorganic composite membranes [12–18]. So far, the separators used in commercial Li-ion batteries are nearly exclusively micro-porous polymer membranes. But they are expensive because the technology of manufacturing is currently controlled by only several companies. The cost of the separator can be over 20% of the total cost of a lithium-ion battery. Therefore, it is important to find alternative, cheap and dependable membrane materials to replace the current commercial separators in order to reduce the cost of the lithium-ion batteries. In this paper, we attempt for the first time to use a commercial rice paper (RP) as the separator membrane in lithium-ion batteries.

The RP was invented over a thousand years ago by Chinese people for traditional Chinese painting and calligraphy. In fact, it is not made from rice but made from a certain plant such as bamboo. In terms of structure, the RP membrane is a fibrous mat-like

membrane so that it has a porous structure and good ability of absorbing of water or liquid, which are exactly two important features required for a separator membrane in a lithium-ion cell. The results of this study indicate that the RP membrane is electrochemically compatible with several widely used or investigated electrode materials and an electrolyte solution for lithium-ion batteries and the cells with the RP membrane as the separator show good electrochemical performance.

2. Experimental

A commercial RP membrane (Taoji Rice Paper Co., Anhui) was purchased and stored in a drier (Dry-498XE, Ace Dragon Co.) at room temperature and under a relative humidity of less than 5%. A commercial separator (Celgard 2400) was also chosen for comparison. Both of them were punched into round discs with a diameter of 16 mm. Meanwhile, some commercial electrode materials including LiFePO_4 (LFP, Nanjing Lithing Co.), LiMn_2O_4 (LMO, Qingdao Qianyun Co.), LiCoO_2 (LCO, Beijing Easpring Co.) and graphite (Zhejiang Jinhe Co.) were selected to prepare electrode laminates. Positive electrode laminates (LFP, LMO and LCO) were prepared by mixing 84 wt% active electrode materials, 8 wt% acetylene black and 8 wt% poly(vinylidene difluoride) (PVDF) in 1-methyl-2-pyrrolidinone (NMP) into slurries and then casting them on an aluminum foil. A negative electrode (graphite) laminate was prepared by mixing 90 wt% graphite and 10 wt% PVDF in NMP into a slurry and casting it on a copper foil. These laminates were all dried at 120 °C for at least 2 h and then punched into discs with a diameter of 14 mm. All the separators and electrode discs were

* Corresponding author. Tel.: +86 551 3606971.

E-mail address: cchchen@ustc.edu.cn (C.H. Chen).

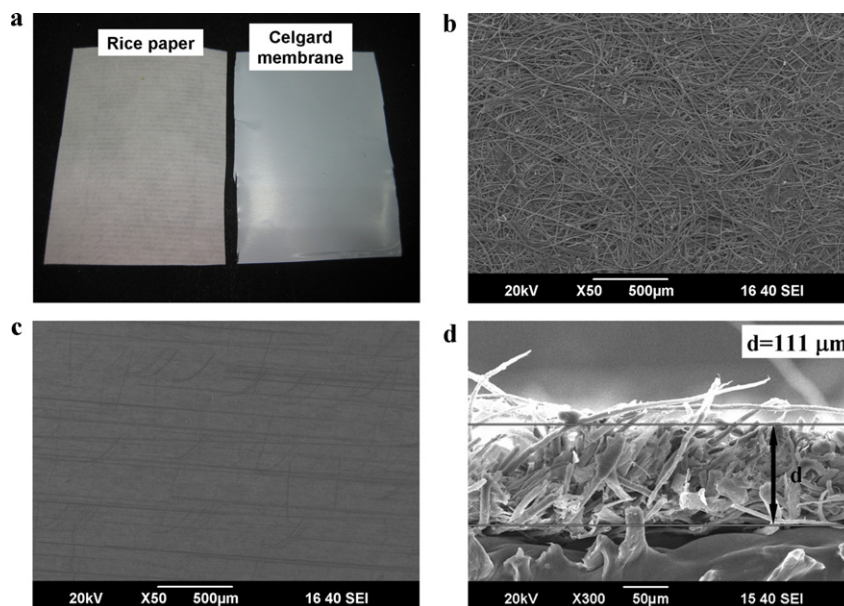


Fig. 1. Photograph of the RP membrane and Celgard separator (a), SEM micrographs of the RP membrane (b) and Celgard separator (c), SEM micrograph of the cross-section (d) of the RP membrane.

treated for 5 hours in a vacuum drying chamber at 80 °C to get rid of absorbed water before being used to assemble the cells.

Coin-cells (CR2032 size) were assembled in an argon-filled glove box with above electrode laminates as working electrodes, Li metal as the counter electrode, and 1 M LiPF₆ in ethylene carbonate (EC):diethyl carbonate (DEC) (1:1, w/w) as the electrolyte. The separators were either a layer of Celgard 2400 or one to four layers of the RP membrane. In one case, a full cell with LFP as the positive and graphite as the negative electrodes was also assembled.

The cells were tested on a multi-channel battery test system (NEWARE BTS-610) with galvanostatic charge and discharge in different selected voltage ranges. Cyclic voltammetry (CV) and AC impedance spectroscopy measurements on the cells were performed with a CHI 604B electrochemical workstation. For the latter, the cells were first cycled galvanostatically at 0.2 C rate for 3 cycles.

The microstructure of the RP membrane was observed under a scanning electron microscope (SEM, Hitachi X-650). The mechanical properties of the RP and Celgard 2400 were measured with a DMAQ800 dynamic mechanical analyzer (TA Instruments) using a mini-tensile bar. The tests to measure the stress–strain relationship were carried out at room temperature, while the tests to measure the thermal shrink of both membranes were conducted at 90 °C.

The RP membrane was also analyzed by infrared (IR) spectroscopy (Bruker TENSOR27).

3. Results and discussion

Fig. 1 shows the photograph and SEM micrographs of the RP membrane and Celgard separator. The Celgard membrane is very smooth while the RP looks rougher with its texture visible even by naked eyes (Fig. 1a). The SEM micrographs (Fig. 1b and c) of the RP and the Celgard membrane show that the RP membrane mainly consists of tortuous cellulose fibers with diameters of 5–40 μm, while the Celgard membrane is much smoother. Note that the scratches on the photo may come from the sample preparation process for the SEM test. The thickness of the RP membrane is about 100 μm (Fig. 1d). The RP membrane may be viewed as a kind of non-woven fabric mat. It has a highly porous structure which is beneficial for the electrolyte to infiltrate into and for the ions to

transport through it. Hence the RP membrane is promising to be used as a separator in lithium-ion batteries.

Fig. 2 shows the stress–strain curves of both membranes in two perpendicular directions. For the RP, the directions are in parallel with and perpendicular to the stripes (Fig. 1a). For the Celgard membrane, the directions are in parallel with and perpendicular to the rolling direction. Although the maximum stress of the RP membrane is about 13.8 and 8.5 MPa in both directions, respectively, while that of Celgard membrane is about 89.2 and 47.7 MPa, respectively. This means that the tensile strength of the RP is poorer than the Celgard membrane. Hence precaution should be exercised when manufacturing a battery using the RP as the separator. On the other hand, the Young's modulus, which is represented by the slope of a curve, of the RP membrane is higher than that of the Celgard membrane. This feature of the RP is advantageous to remain stable for the separator when it is soaked with liquid electrolyte, preventing the separator from degradation that may cause internal short circuiting of a battery.

Fig. 3 shows the strain of the RP and the Celgard membranes kept at 90 °C for over 60 min. Following the increase of the temperature to 90 °C, the strain of the RP membrane in both directions exhibits

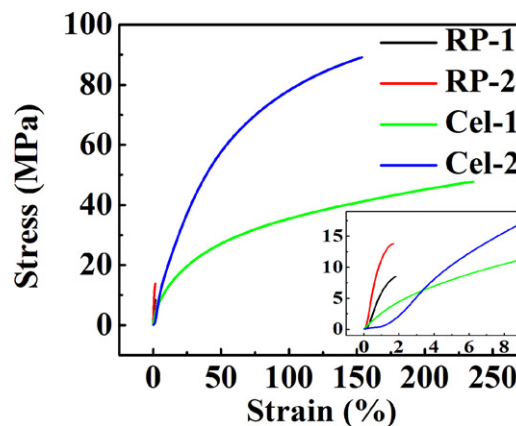


Fig. 2. Stress–strain curves of the RP and Celgard (Cel) membranes in both directions.

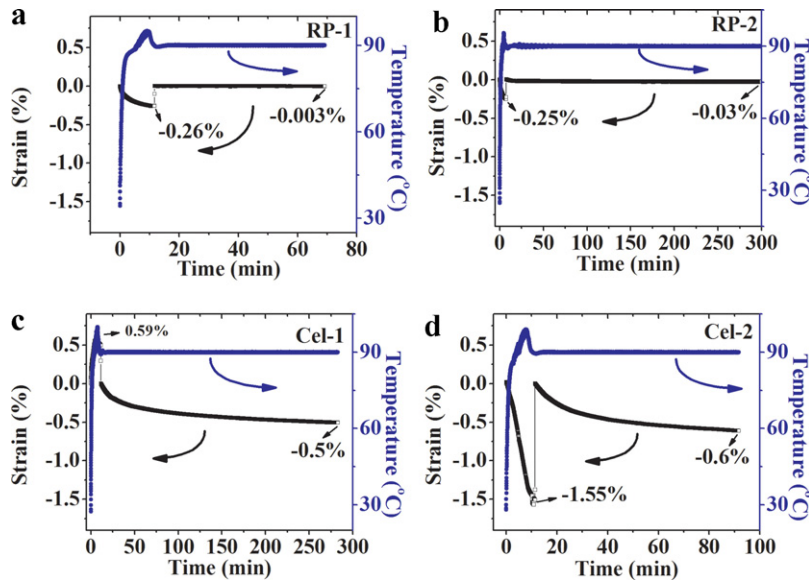


Fig. 3. Strain of the RP (a and b) and Celgard (c and d) membranes in both directions at 90 °C for over 60 min.

a low rate of shrinkage of -0.26% (Fig. 3a) and -0.25% (Fig. 3b), respectively. The Celgard membrane shows an opposite behavior in two perpendicular directions in that it shrinks by -1.55% in one direction (Fig. 3c) and expands first by 0.59% and then shrinks in the other direction (Fig. 3d). After the temperature reaches $90\text{ }^{\circ}\text{C}$ and keeps unchanged, the dimension change of the RP membrane in both directions is almost ignorable, being -0.003% and -0.03% , respectively (Fig. 3a and b). To the contrary, the strain of the Celgard membrane in both directions has a sustained shrinkage of -0.5% after 270 min (Fig. 3c) and -0.6% after 300 min (Fig. 3d). Such shrinkage may lead to the direct contact of the positive and negative electrodes and thus poses a safety issue of a battery.

Fig. 4 shows the IR spectrum of the rice paper. It is similar to the IR spectrum of another plant fiber [19]. Following bands can be observed and assigned in the spectrum: O–H stretch ($\sim 3400\text{ cm}^{-1}$), C–H stretch in methyl and methylene groups ($\sim 2900\text{ cm}^{-1}$), C=O stretch ($\sim 1650\text{ cm}^{-1}$), aromatic skeletal vibrations combined with C–H in plane deformation ($\sim 1427\text{ cm}^{-1}$), C–H deformation vibration ($\sim 1375\text{ cm}^{-1}$), O–H plane deformation vibration ($\sim 1337\text{ cm}^{-1}$), CH_2 rocking vibration ($\sim 1318\text{ cm}^{-1}$), C–O–C asymmetric valence vibration ($\sim 1163\text{ cm}^{-1}$), asymmetric in-phase ring stretching, C–C and C–O stretching ($\sim 1114\text{ cm}^{-1}$), C–O valence vibration ($\sim 1059\text{ cm}^{-1}$), C–O ether vibrations ($\sim 1034\text{ cm}^{-1}$),

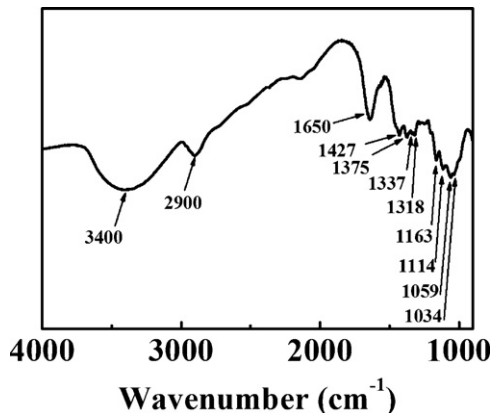


Fig. 4. The IR spectrum of the rice paper.

respectively. There is no obvious evidence for the existence of water in the rice paper.

A suitable separator should be stable in the voltage ranges where a battery is operating. Fig. 5 shows the cyclic voltammograms (CV) for the cells with the RP and Celgard membranes as the separators, stainless steel (SS) as the working electrode and a lithium metal as the counter and reference electrodes at a scanning rate

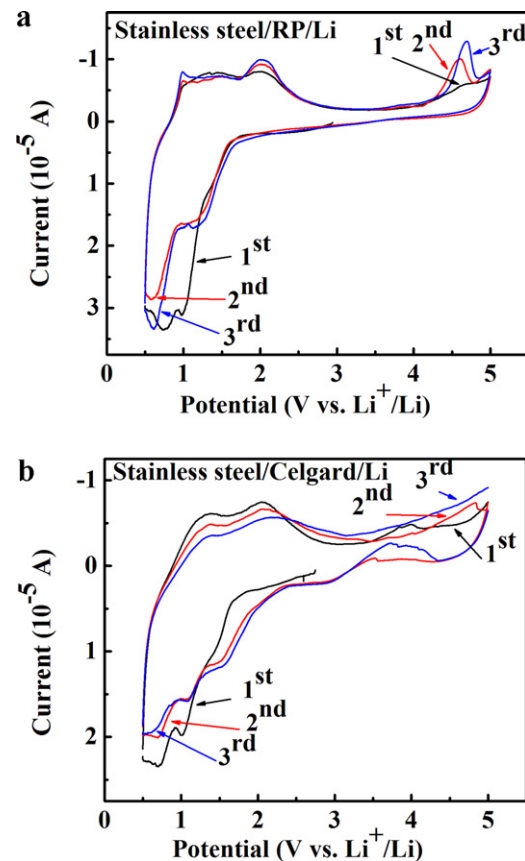


Fig. 5. The cyclic voltammograms (CV) for the cells with the RP and Celgard membrane as separators, stainless steel (SS) as working electrode and a lithium metal as counter and reference electrodes. The scanning rate was 0.2 mV s^{-1} during $0.5\text{--}5.0\text{ V}$.

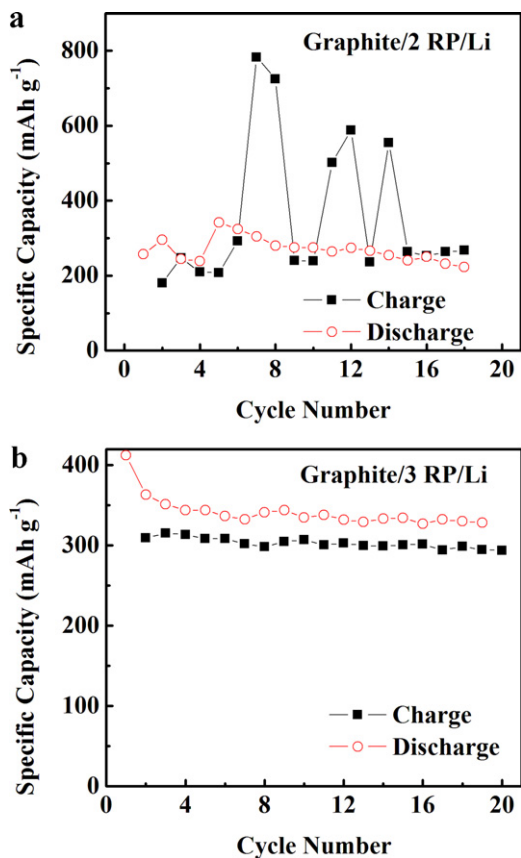


Fig. 6. Cycling performance of Li/graphite cells with 2 (a) or 3 (b) layers of the RP membrane as separator. The n in “ n RP” or “ n Celgard” means the number of membrane layers.

of 0.2 mV s^{-1} in the voltage range of 0.5–5.0 V. It can be seen that in the voltage range of 0.5–2.5 V, the CV curves of the two cells are similar, meaning that the peaks observed are probably related to

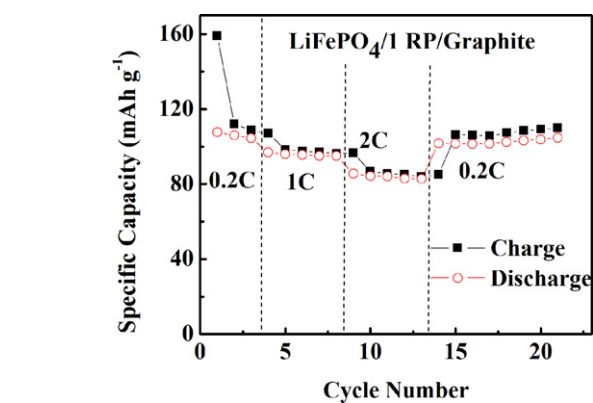
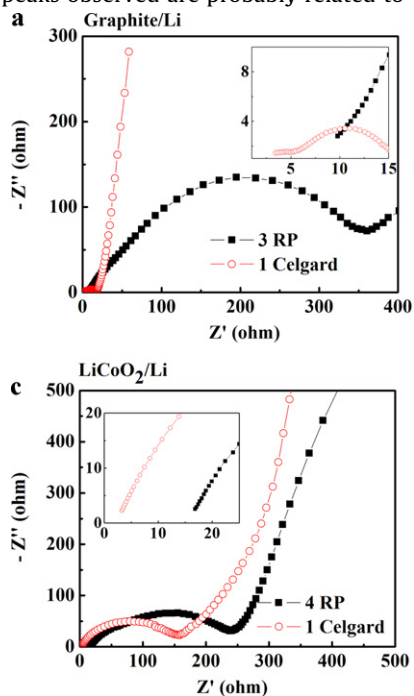


Fig. 7. A graphite/LFP full cell with one layer of the RP membrane as the separator.

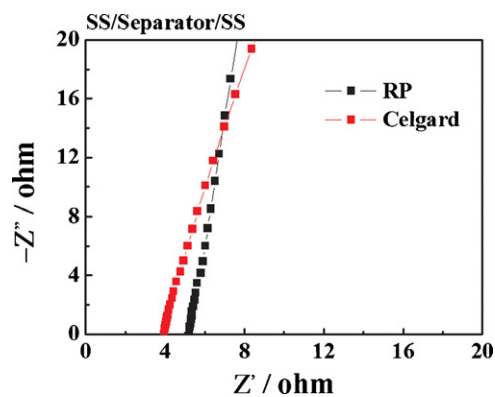


Fig. 9. The AC impedance spectra of symmetric cells SS/separator/SS with rice paper and Celgard separator as separator.

the redox reactions of some metal oxides (e.g. NiO and Fe_2O_3) on the surface of SS. These peaks have nothing to do with the separators RP and Celgard. In the voltage of 4.4–5.0 V, an oxidation peak appears

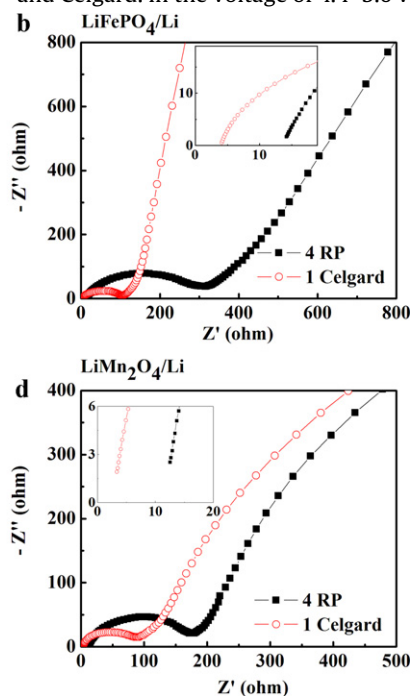


Fig. 8. The AC impedance spectra of the half-cells with graphite (a), LiFePO_4 (b), LiCoO_2 (c) and LiMn_2O_4 (d) as the working electrodes. All the cells were first cycled galvanostatically at 0.2 C rate for 3 cycles (the rate n C means the applied current at which a fully charged cell would be completely discharged in $1/n$ h). The insets graphs show the zoom-in spectra.

at 4.5 V since the second cycle for the Li/RP/SS cell (Fig. 5a), while no oxidation peak is observed for the Li/Celgard/SS cell (Fig. 5b). This suggests that the RP may be gradually oxidized at the potentials above 4.5 V vs. Li⁺/Li. Therefore, the RP is electrochemically stable when the upper voltage limit is below 4.5 V, which is the case for most of the lithium-ion batteries.

Fig. 6 shows the cycling performances of Li/graphite cells using different number of layers of the RP as the separator. When only 1 or 2 layers of the RP membrane are used as the separator, overcharge phenomenon is observed during the cycling process (Fig. 6a). Nevertheless, the overcharged cell seems to be able to recover by itself. When 3 layers of the RP membrane are used, the cell can cycle successfully without any overcharge (Fig. 6b). The possible reason may be related to the growth of the dendritic lithium which may pierce 2 layers of the RP membrane to cause short-circuiting during the charge process. But when the dendritic lithium is fused during the short-circuiting, the cell can recover to normal again. It seems that 3 layers of RP membrane are thick enough to suppress the growth of dendritic lithium so that the cell would not be overcharged. To examine this proposition, a graphite/LFP full cell with only one layer of RP membrane as the separator is assembled and tested (Fig. 7). No overcharge phenomenon appears during the cycling, which means that only one layer of the RP membrane is enough for the cell to cycle successfully when the negative electrode is not Li metal.

AC impedance spectroscopy was used to obtain information on the resistivity of the electrolyte solution in the RP membrane. Fig. 8 shows the AC impedance spectra of the half cells with LFP, LCO, LMO or graphite as the working electrodes, and the RP or Celgard membranes as the separators. The intercepts of the impedance spectra at the real axis represent the resistances (R_s) of the electrolyte solution in the pores of the separator. As shown in Fig. 8, the cells with 3 or 4 layers of the RP membrane show higher R_s (10–17 ohm) than the cells with a single layer of Celgard membrane (3–5 ohm). The difference is possibly caused by the difference in total thickness and microstructures of the separators. The value of R_s can be given by the following expression [20]:

$$R_s = \frac{\rho_s L}{A} \left(\frac{\tau}{f} \right)$$

where ρ_s is the resistivity of the electrolyte, A is the geometric area of the electrode, L is the thickness of the separator, τ is tortuosity (the ratio between the path length of the ions and the thickness of the separator), and f is pore fraction (the ratio between the pore volume and the total geometrical volume of the separator). The ratio τ/f can actually indicate how easy it is for the electrolyte to penetrate through a separator membrane. The thickness (L) of the Celgard separator is 25 μm , while that of the RP membrane (1 layer) is 100 μm . As mentioned above, the value of R_s for the measured cells with 3–4 layers of the RP as the separators is approximately 4 times as large as for the cells with one layer of Celgard separator (Fig. 8). Because the values of ρ_s and A are the same for the two kinds of cells and the total thickness of 3–4 layers of RP membrane is about 16 times of 1 layer of Celgard, the τ/f value for the RP membrane is only about one fourth that of the Celgard separator. It means that the RP membrane will give rise to a lower resistance than the Celgard separator of the same thickness. The ionic conductivities of electrolyte in the rice paper and the Celgard separator with two symmetric cells SS/separator/SS are shown in Fig. 9. The conductivity can be calculated with $\sigma = L/AR$, where L and A are the thickness and the geometric area of the separator, respectively, while R is the total resistance of the electrolyte across the membranes. As mentioned above, the thicknesses of RP and Celgard separator are about 100 and 25 μm , respectively. So that the value of σ_{RP} is about 3 times of σ_{Celgard} . It means that the practical ionic conductivity of electrolyte across the RP is higher than that across the Celgard separator.

Fig. 10 shows the comparison of cycling performances of four lithium cells with different working electrodes versus Li. There are virtually no remarkable differences in the cell performance between RP and Celgard cells although the Li/graphite cell using RP indeed shows slightly better capacity retention than that with Celgard separator (Fig. 10a). The difference might be due to some experimental errors. When the working electrode materials are LFP, LCO and LMO (Fig. 10b–d), the discharge capacities of the cells with the RP membrane as the separator are still comparable with those with the Celgard separator at 0.2C, 1C, and 2C. Especially at low rates, the lower the rate is, the higher capacity the batteries with

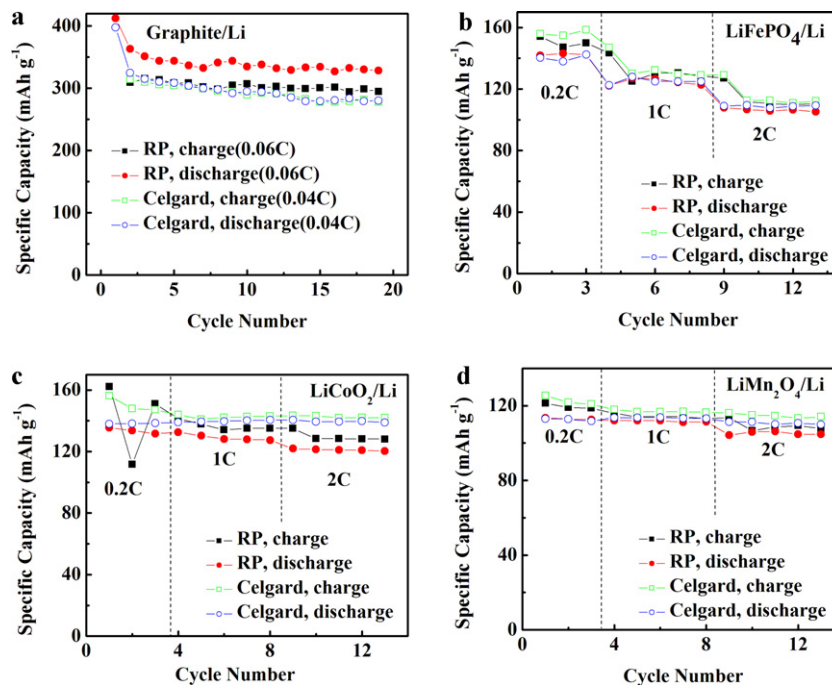


Fig. 10. The cycling performances of four half-cells with different working electrodes versus Li: graphite (a), LiFePO₄ (b), LiCoO₂ (c) and LiMn₂O₄ (d).

the RP membrane as the separator can deliver. This means that the RP membrane as a separator is particularly interesting for some low power applications such as smart mobile phones and notebook computers.

4. Conclusions

This study is the first demonstration of the use of a commercial RP in lithium-ion batteries. The batteries with RP separator exhibit good electrochemical performance at low rates. Several kinds of electrode materials including graphite, LFP, LCO and LMO are proved to be compatible with the stability of the RP separator. Besides, the thermal stability of the RP membrane at 90 °C is superior to the commercial separator. Owing to its wonderful flexibility, high porosity, low cost and acceptable electrochemical performance, the RP membrane has a strong chance to be applied in lithium-ion batteries to partially replace other commercial separators.

Acknowledgments

This study was supported by National Science Foundation of China (grant nos. 20971117, 10979049 and J1030412) and Education Department of Anhui Province (grant no. KJ2009A142). We are also grateful to the Solar Energy Operation Plan of Academia Sinica.

References

- [1] S.S. Zhang, *J. Power Sources* 164 (2007) 351–364.
- [2] D.R. Lloyd, K.E. Kinzer, H.S. Tseng, *J. Membr. Sci.* 52 (1990) 239–261.
- [3] A. Subramania, N.T.K. Sundaram, A.R.S. Priya, G.V. Kumar, *J. Membr. Sci.* 294 (2007) 8–15.
- [4] S.S. Zhang, K. Xu, D.L. Foster, M.H. Ervin, T.R. Jow, *J. Power Sources* 125 (2004) 114–118.
- [5] Y.H. Ding, P. Zhang, Z.L. Long, Y. Jiang, F. Xu, W. Di, *J. Membr. Sci.* 329 (2009) 56–59.
- [6] A.I. Gopalan, P. Santhosh, K.M. Manesh, J.H. Nho, S.H. Kim, C.G. Hwang, K.P. Lee, *J. Membr. Sci.* 325 (2008) 683–690.
- [7] J.R. Kim, S.W. Choi, S.M. Jo, W.S. Lee, B.C. Kim, *Electrochim. Acta* 50 (2004) 69–75.
- [8] Y.M. Lee, N.S. Choi, J.A. Lee, W.H. Seol, K.Y. Cho, H.Y. Jung, J.W. Kim, J.K. Park, *J. Power Sources* 146 (2005) 431–435.
- [9] Y.M. Lee, J.W. Kim, N.S. Choi, J.A. Lee, W.H. Seol, J.K. Park, *J. Power Sources* 139 (2005) 235–241.
- [10] M.K. Song, Y.T. Kim, J.Y. Cho, B.W. Cho, B.N. Popov, H.W. Rhee, *J. Power Sources* 125 (2004) 10–16.
- [11] N.T.K. Sundaram, A. Subramania, *J. Membr. Sci.* 289 (2007) 1–6.
- [12] H.S. Jeong, S.C. Hong, S.Y. Lee, *J. Membr. Sci.* 364 (2010) 177–182.
- [13] K.M. Kim, N.G. Park, K.S. Ryu, S.H. Chang, *Electrochim. Acta* 51 (2006) 5636–5644.
- [14] Y.H. Liao, M.M. Rao, W.S. Li, L.T. Yang, B.K. Zhu, R. Xu, C.H. Fu, *J. Membr. Sci.* 352 (2010) 95–99.
- [15] P.P. Prosini, P. Villano, M. Carewska, *Electrochim. Acta* 48 (2002) 227–233.
- [16] D. Takemura, S. Aihara, K. Hamano, M. Kise, T. Nishimura, H. Urushibata, H. Yoshiyasu, *J. Power Sources* 146 (2005) 779–783.
- [17] S.S. Zhang, K. Xu, T.R. Jow, *J. Solid State Electrochem.* 7 (2003) 492–496.
- [18] S.S. Zhang, K. Xu, T.R. Jow, *J. Power Sources* 140 (2005) 361–364.
- [19] M. Schwanninger, J.C. Rodrigues, H. Pereira, B. Hinterstoisser, *Vib. Spectrosc.* 36 (2004) 23–40.
- [20] L.B. Hu, H. Wu, F. La Mantia, Y.A. Yang, Y. Cui, *ACS Nano* 4 (2010) 5843–5848.